

Influence of Some Thiadiazole Derivatives on Corrosion Inhibition of Mild Steel in Formic and Acetic Acid Media

M.Z.A. Rafiquee,^a S. Khan,^{a,*} N. Saxena,^a M.A. Quraishi^b

^a Corrosion Research Laboratory, Department of Applied Chemistry, Faculty of Engineering and Technology, Aligarh Muslim University, Aligarh-202 002, India

^b Department of Applied Chemistry, Institute of Technology, Banaras Hindu University, Varanasi, India

Received 30th April 2007; accepted 17th July 2007

Abstract

2-amino-1, 3, 4-thiadiazoles (AT), 2-amino-5-methyl-1, 3, 4-thiadiazoles (AMT), 2-amino-5-ethyl -1, 3, 4-thiadiazoles (AET) and 2-amino-5-propyl -1, 3, 4-thiadiazoles (APT) were synthesized. FT-IR and NMR studies were done in order to confirm the composition of the synthesized inhibitors. These compounds were evaluated as inhibitors for mild steel in 20% formic acid and 20% acetic acid by weight loss, potentiodynamic polarization and electrochemical impedance techniques. Scanning electron microscopic study (SEM) was also used to investigate the surface morphology of inhibited and uninhibited metal samples. The inhibition efficiency of these compounds was found to vary with the inhibitor concentration, immersion time, temperature and acid concentration. The adsorption of these compounds on the steel surface from both acids were found to obey Langmuir's adsorption isotherm. These compounds are mixed type inhibitors in both acid solutions. Various thermodynamic parameters (E_a , ΔG_{ads} , ΔQ , ΔH , ΔS , $t_{1/2}$) have also been calculated to investigate the mechanism of corrosion inhibition. Electrochemical impedance study was used to investigate the mechanism of corrosion inhibition.

Keywords: mild steel, potentiodynamic polarization, thiadiazoles, FT-IR spectroscopy, Langmuir adsorption isotherm, scanning electron microscopy.

Introduction

Corrosion studies on metals in organic acid solutions are scarce in comparison with similar studies in mineral acids [1-4]. The presence of reactive carboxyl group $-\text{COOH}$ in organic acids makes them a basic building block for many compounds such as drugs, pharmaceuticals, plastics and fibers.

* Corresponding author. E-mail address: sadaf_khan5@rediffmail.com

Few corrosion studies of these acids [5-8] have been made. However, at high temperatures, the acids can dissociate, forming more aggressive ions that can cause faster corrosion than might otherwise be expected.

A variety of organic compounds containing heteroatoms such as O, N, S and multiple bonds in their molecule are of particular interest as they give better inhibition efficiency than those containing N or S alone [9-13], as lone pair of electrons present on heteroatoms are the important structural features that determine the adsorption of these molecules on the metal surface.

The corrosion inhibiting behaviour of thiadiazoles on mild steel was reported in acidic media [14-17].

In the present investigation the influence of four thiadiazoles, namely, 2-amino-1, 3, 4-thiadiazoles (AT), 2-amino-5-methyl-1, 3, 4-thiadiazoles (AMT), 2-amino-5-ethyl -1, 3, 4-thiadiazoles (AET) and 2-amino-5-propyl -1, 3, 4-thiadiazoles (APT) on corrosion inhibition of mild steel in 20% formic acid and 20% acetic acid with the minimum corrosion rate [18], were undertaken with a view to establish their corrosion inhibition efficiencies along with the mechanism involved on their adsorption phenomenon.

Experimental

Material preparation

AR grade formic and acetic acid (MERCK) and doubled distilled water were used for preparing test solutions of 20% formic acid and 20% acetic acid for all the experiments. The inhibitors were synthesized following a procedure described earlier [19] and compounds were characterized through their spectral data and their purity was confirmed by thin layer chromatography (TLC), FT-IR and NMR study. Name and structural formulas of the condensation products are given in Table 1.

FT-IR spectroscopy

FT-IR spectroscopic study was used to investigate the purity of the compound synthesized. The results are listed below:

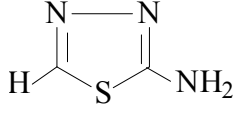
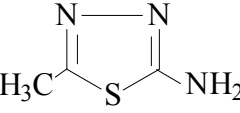
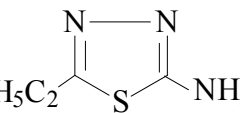
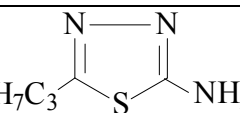
1. 2-amino-1, 3, 4-thiadiazoles (AT) - IR (KBr): 3348 (NH₂), 1647 (C=N), 1311 (C-N), 600 (C-S) cm⁻¹.
2. 2-amino-5-methyl-1, 3, 4-thiadiazoles (AMT) - IR (KBr): 3321 (NH₂), 1645 (C=N), 1316 (C-N), 650 (C-S), 1284 (CH₃-) cm⁻¹.
3. 2-amino-5-ethyl-1, 3, 4-thiadiazoles (AET) - IR (KBr): 3220 (NH₂), 1642 (C=N), 1316 (C-N), 653 (C-S), 1002 (CH₃CH₂-) cm⁻¹.
4. 2-amino-5-propyl-1, 3, 4-thiadiazoles (APT) - IR (KBr): 3044 (NH₂), 1653(C=N), 1285 (C-N), 657(C-S), 800 (CH₃CH₂CH₂-) cm⁻¹.

NMR spectroscopy

NMR spectral data (δ CDCl₃)

2-amino-5-propyl-1, 3, 4-thiadiazoles (APT) - 0.983 (3H, CH₃), 2.008 (4H, (CH₂)₂), 2.816 (2H, NH₂)

Table 1. Name and abbreviations of the compound used.

S.No	Structure	Designation and abbreviation
1		2-amino-1, 3, 4- thiadiazole, AT
2		5-methyl-2- amino-1, 3, 4- thiadiazole, AMT
3		5-ethyl-2-amino-1, 3, 4- thiadiazole, AET
4		5-propyl-2-amino-1, 3, 4- thiadiazole, APT

Weight loss measurement

The mild steel samples having composition, (Wt %): 0.14% C, 0.35% Mn, 0.17% Si, 0.025% S, 0.03% P and balance Fe has been used for the experiment. Mild steel samples of size 2.0 cm × 2.0 cm × 0.025 cm were used for weight loss measurement studies. Weight loss measurement studies were carried out at various temperatures ranging from 30 to 60 °C for various immersion times from 24 to 120 hrs. The experiments were performed as per ASTM method described previously [20]. The inhibition efficiency of the inhibitors was calculated by using the following equation:

$$IE = (CR_0 - CR_i) \times 100 / CR_0 \quad (1)$$

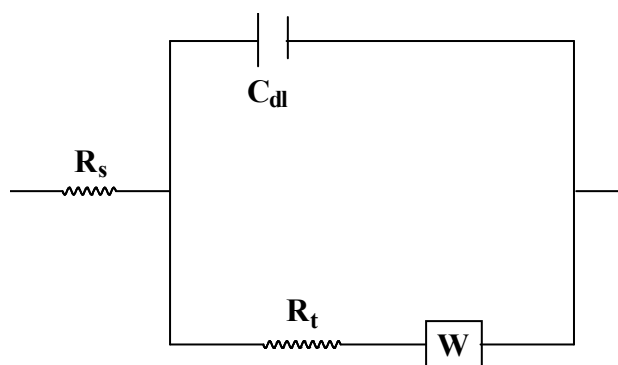
where CR_0 = corrosion rate of blank (formic and acetic acid) and CR_i = corrosion rate after adding inhibitors.

Electrochemical studies

For potentiodynamic polarization studies of mild steel, strips of the above composition, coated with commercially available lacquer with an exposed area of 1.0 cm² were used and the experiments were carried out at temperature (30 ± 1 °C). Time taken to steady state potential values of the specimens was 30 minutes. Sweep rate in potentiodynamic experiment was 1 mV/sec. Potentiodynamic polarization studies were carried out using an EG & G Princeton Applied Research (PAR) potentiostat / galvanostat (model 173), a universal programmer (model 175) and an X-Y recorder (model RE0089). A platinum foil was used as auxiliary electrode and a saturated calomel electrode (SCE) was used as reference electrode.

Electrochemical impedance studies

The electrical equivalent circuit for the system is shown in the figure below:



R_s = solution resistance, R_t = charge transfer resistance, W = Warburg impedance, C_{dl} = double layer capacitance.

The values of R_t and C_{dl} were obtained using the Nyquist plot [21]. The %IE was calculated using equation [22]:

$$IE \% = \frac{1/R_o - 1/R_t}{1/R_{t0}} \times 100 \quad (2)$$

where R_t and R_{t0} are the charge transfer resistance with and without inhibitor, respectively.

The impedance diagrams are not perfect semicircles, and this difference has been attributed to frequency dispersion [23]. All the measurements were carried out using Zahner IM-6 electrochemical workstation at 30 ± 2 °C, at a frequency range of 5 Hz –100k Hz at E_{corr} for mild steel in 20% formic acid at different inhibitor concentration.

Scanning electron microscopy

Scanning electron microscope (SEM) model No 435 VP LEO, was used to study the morphology of the corroded surface in the presence and absence of the inhibitors. After weight loss studies at 30 °C for 24 hours the specimens were thoroughly washed with double distilled water before examination. The photographs have been taken from that portion of specimen from where better information was obtained. They were photographed at appropriate magnifications (2500-3000 micron). To understand the morphology of the steel surface in absence and presence of the inhibitors, the following cases have been examined:

- i) polished mild steel specimen;
- ii) mild steel specimen dipped in 20% formic acid;
- iii) mild steel specimens dipped in 20% formic acid containing 500-ppm concentrations of APT inhibitors.

Results and discussion

Weight loss measurements

The values of percentage inhibition efficiency (%IE) and corrosion rate (CR) obtained from weight loss method at different concentrations at 30 °C are summarized in Table 2. All compounds inhibit corrosion of mild steel in formic and acetic acid solution, at all concentrations used in the study, i.e., 10 ppm – 100 ppm. It has also been observed that the inhibition efficiency for all these compounds increases with the increase in concentration, as shown in Fig. 1a and Fig. 2a.

Table 2. Corrosion parameters for mild steel in aqueous solution of 20% formic acid and 20% acetic acid in absence and presence of different concentrations of various inhibitors from weight loss measurements at 30 °C for 24 h.

Inhibitor conc. (ppm)	20% formic acid			20% acetic acid		
	Weight loss (mg)	IE (%)	CR (mmpy)	Weight loss (mg)	IE (%)	CR (mmpy)
Blank	308.21	-	34.10	150.36	-	7.44
AT						
10	108.04	64.95	5.02	58.43	61.13	2.71
25	100.34	67.44	4.66	50.16	66.64	2.33
50	87.45	71.62	4.06	42.20	71.93	1.96
75	69.20	77.54	3.21	38.50	74.39	1.79
100	63.40	79.42	2.94	31.40	79.12	0.46
AMT						
10	89.68	70.92	4.16	41.03	72.71	1.91
25	75.03	75.65	3.48	36.95	75.43	1.72
50	60.85	80.26	2.82	32.87	78.14	1.53
75	49.63	83.89	2.30	29.04	80.68	1.35
100	46.09	85.05	2.14	26.13	82.62	1.21
AET						
10	59.08	80.83	2.74	38.65	74.29	1.79
25	57.17	81.45	2.65	34.07	77.34	1.58
50	47.93	84.44	2.23	27.53	81.69	1.28
75	41.39	85.59	1.92	22.84	84.80	1.06
100	39.52	87.18	1.84	19.60	86.96	0.91
APT						
10	48.86	84.15	2.27	35.85	76.15	1.66
25	42.93	86.07	2.09	30.12	79.96	1.40
50	39.65	87.14	1.84	24.71	83.56	1.15
75	30.26	90.18	1.41	19.52	87.02	0.91
100	24.15	92.16	1.12	14.94	90.06	0.69

It is observed that the tested thiadiazoles show a decrease in the inhibition efficiency with immersion time from 24 to 120 hours in formic as well as in acetic acid. This shows the desorption of the adsorbed thiadiazoles over a longer test period. Inhibition efficiency of all the compounds against the immersion time is shown in Fig. 1b and Fig. 2b.

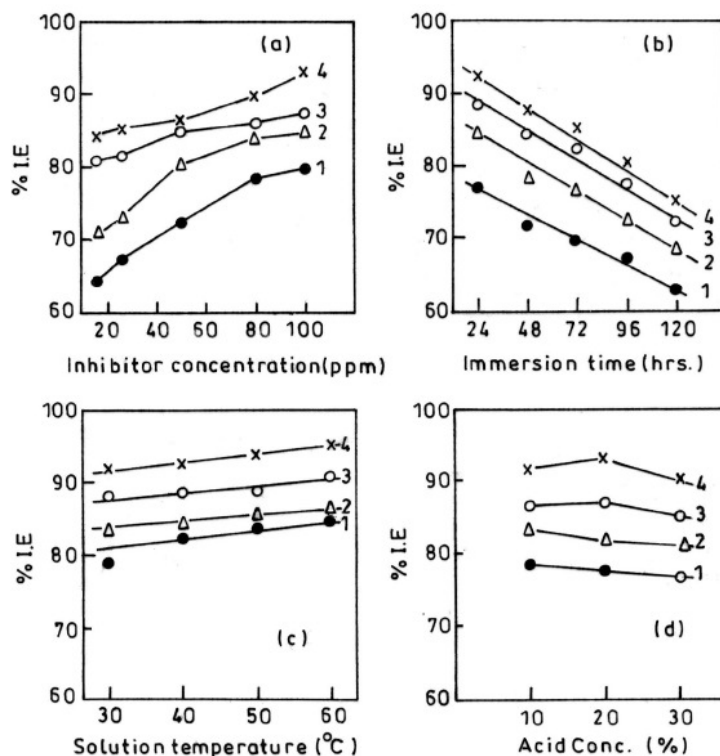


Figure 1. Variation of the inhibition efficiency with (a) inhibitor concentration, (b) immersion time, (c) solution temperature, (d) acid concentration in 20% formic acid (1: AT; 2: AMT; 3: AET; 4: APT).

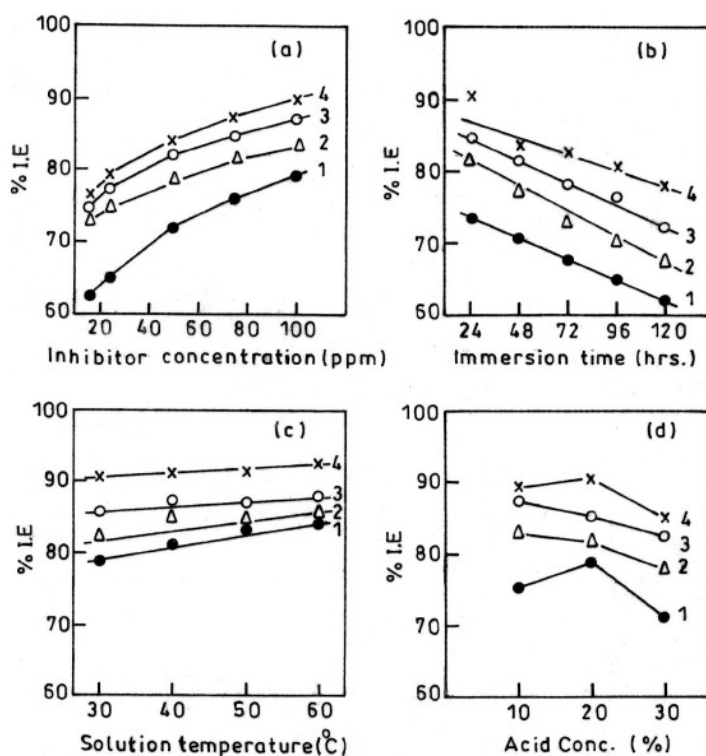


Figure 2. Variation of the inhibition efficiency with (a) inhibitor concentration, (b) immersion time, (c) solution temperature, (d) acid concentration in 20% acetic acid (1: AT; 2: AMT; 3: AET; 4: APT).

IE for compounds such as AT, AMT, AET and APT increases with temperature from 30 °C to 60 °C (Fig. 1c and Fig. 2c), indicating that the inhibitive film formed on the metal surface is protective up to 60 °C. From Fig. 1d and Fig. 2d, it is clear that change in acid concentration from 10% to 30% did not cause any significant change in inhibition efficiency of all the compounds, thereby suggesting that all the compounds are effective corrosion inhibitors in acid solution at different concentrations.

The degree of surface coverage (θ) for different inhibitor concentrations in 20% formic acid and 20% acetic acid at 30 °C over 24-hour immersion time was evaluated from weight loss values. The data were tested graphically by fitting to various isotherms. A plot of $\log (\theta / 1 - \theta)$ versus $1/T$ is shown in Fig. 3a and Fig. 4a. The plot gives the values of heat of adsorption (Q), which is determined from the slope ($-Q/2.303R$). The values of heat of adsorption are presented in Table 3. The values of heat of adsorption for the inhibitors in formic and acetic acid are found to be less than (-40 kJ mol^{-1}). This indicates that all the inhibitors are adsorbed physically [24].

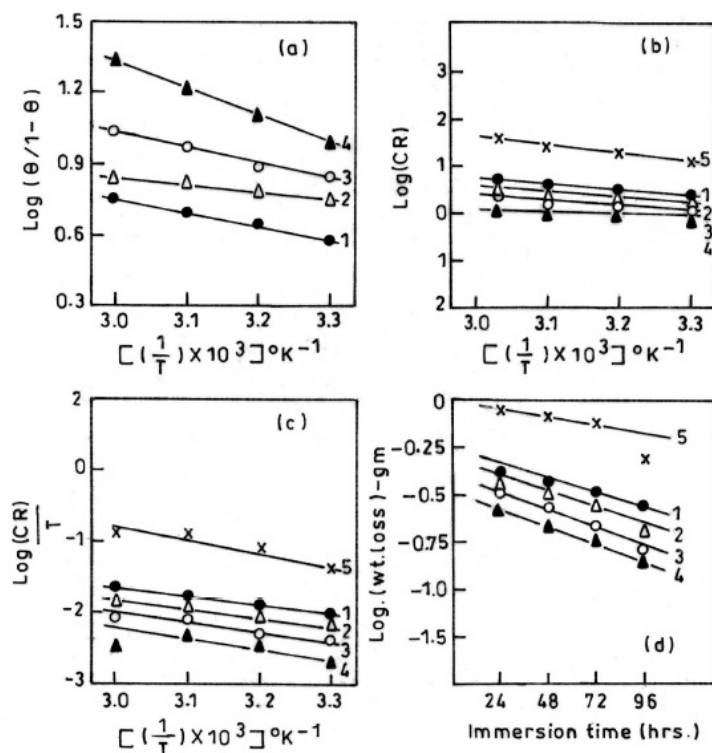


Figure 3. (a) Adsorption isotherm plot for $\log (\theta / 1 - \theta)$ versus $1/T$; (b) adsorption isotherm plot for $\log (CR)$ versus $1/T$; (c) adsorption isotherm plot for $\log (CR/T)$ versus $1/T$; and (d) half-life plot for $\log (\text{weight loss})$ versus immersion time in 20% formic acid (1: AT; 2: AMT; 3: AET; 4: APT; 5: Blank).

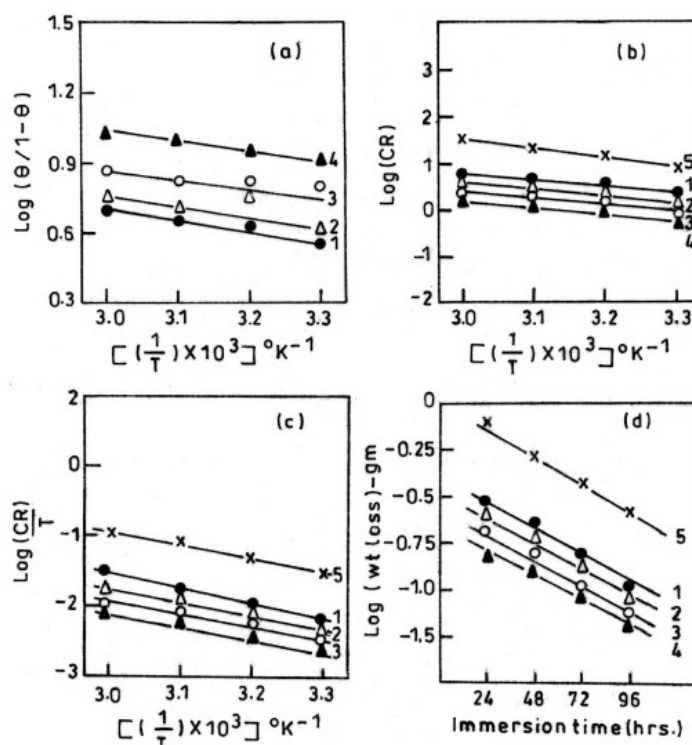


Figure 4. (a) Adsorption isotherm plot for $\log (\theta / 1-\theta)$ versus $1/T$; (b) adsorption isotherm plot for $\log (CR)$ versus $1/T$; (c) adsorption isotherm plot for $\log (CR/T)$ versus $1/T$; and (d) half-life plot for $\log (\text{weight loss})$ versus immersion time in 20% acetic acid (1: AT; 2: AMT; 3: AET; 4: APT; 5: Blank).

Table 3. Thermodynamic activation parameters for mild steel in 20% formic acid and 20% acetic acid in absence and presence of inhibitors of 100-ppm concentration.

Inhibitor conc. (ppm)	E_a (KJ mol ⁻¹)	ΔH (KJ mol ⁻¹)	$-\Delta S$ (J mol ⁻¹ K ⁻¹)	$-\Delta G_{\text{ads}}$ (KJ mol ⁻¹)	$-Q$ (KJmol ⁻¹)
20% formic acid	31.91	140.41	212.91	—	—
AT	19.15	25.52	229.18	32.78	19.15
AMT	12.76	19.15	233.98	34.08	12.76
AET	6.38	6.38	237.89	34.14	6.38
APT	3.19	28.72	242.59	37.08	10.21
20% acetic acid	30.84	102.12	214.83	—	—
AT	25.53	51.06	226.32	32.84	9.57
AMT	31.91	41.49	229.19	33.67	8.94
AET	38.29	31.91	234.93	34.59	2.68
APT	38.29	25.53	239.72	35.83	10.21

It has been reported earlier [25-27] that, in acid solution, the logarithm of the corrosion rate is a linear function of $1/T$ (Arrhenius equation):

$$\log (\text{rate}) = \frac{-E_a^0}{2.303RT} + A \tag{3}$$

where, E_a° is the apparent activation energy, R the general gas constant and A the Arrhenius pre exponential factor. A plot of \log (corrosion rate) versus $1/T$ gave straight lines as shown in Fig. 3b and Fig. 4b. The values of activation energy (E_a°) obtained from the slope of the plot are given in Table III. An alternative formula for the Arrhenius equation in the transition state is:

$$\text{rate} = \frac{RT}{Nh} \exp\left(\frac{\Delta S^{\circ}}{R}\right) \exp\left(-\frac{\Delta H^{\circ}}{RT}\right) \quad (4)$$

where, h is the Plank constant, N the Avogadro's number, ΔS° the entropy of activation, and ΔH° the enthalpy of activation. A plot of $\log (CR/T)$ versus $1/T$ gave a straight line, (Fig. 3c and Fig. 4c) with a slope of $(-\Delta H^{\circ} / 2.303 R)$ and an intercept of $[(\log (R / Nh) + (\Delta S^{\circ} / 2.303 R))]$, from which the values of ΔS° and ΔH° were calculated and are listed in Table III. The data show that the thermodynamic activation functions (E_a°) of the corrosion in mild steel in 20% formic acid in the presence of the inhibitors are lower than those in the free acid solution, indicating that all the inhibitors exhibit high inhibition efficiency at elevated temperatures [28], while the (E_a°) values in the presence of inhibitors in acetic acid are higher than those in the free acid solution, except for AT inhibitor, indicating that the inhibitors exhibit high inhibition efficiency at lower temperatures [28]. The values of ΔH° (Table III) are in the order $AT > AMT > APT > AET$ in formic acid, while $AT > AMT > AET > APT$ in acetic acid, which is an indicative of the order of energy barrier at elevated temperature [28]. The values of activation ΔS° in the absence and presence of the inhibitors are large and negative. This indicates that the activated complex in the rate determining step represents an association rather than a dissociation step, meaning that a decrease in disorderness takes place during the course of transition from reactants to the activated complex [29]. The average values for free energy of adsorption (ΔG_{ads}), calculated using the following equations [30] are given in Table III.

$$\Delta G_{\text{ads}} = - RT \ln (55.5 K) \quad (5)$$

and K is given by:

$$K = \theta / C (1 - \theta) \quad (6)$$

where, θ is degree of coverage on the metal surface, C is the concentration of the inhibitor in mol l^{-1} , K is the equilibrium constant, R is a gas constant and T is the temperature. It is found that the ΔG_{ads} values for the studied compound at higher temperature are less than -40 kJ mol^{-1} , indicating that the thiadiazoles are physically adsorbed on the metal surface [31].

The low and negative value of ΔG_{ads} indicates the spontaneous adsorption of the inhibitor on the surface of mild steel [32].

The plot of log (weight loss) versus immersion time, as shown in Fig. 3d and Fig. 4d, gave a straight line indicating that it follows first order reaction. The value of the rate constant is calculated by using the first order rate law [33]

$$k = \frac{2.303}{t} \log \frac{[A_0]}{[A]} \quad (7)$$

where $[A_0]$ is the initial mass of the metal and $[A]$ is the mass corresponding to time t . The half-life ($t_{1/2}$) values were calculated using the relationship [34]

$$t_{1/2} = 0.693/k \quad (8)$$

The values of rate constants and half-life ($t_{1/2}$) obtained from the above relations are summarized in Table 4. Half-life values were found to be constant at different immersion times. The order of effectiveness of the inhibitors were observed as AET > APT > AMT > AT in 20% formic acid and APT > AET > AMT > AT in 20% acetic acid. The constant values of rate constant further confirmed that the corrosion of mild steel in 20% formic acid and in 20% acetic acid in the presence of different inhibitors follows first order kinetics.

Table 4. Half-life (h) values for the corrosion of mild steel at different immersion times in 20% formic acid and 20% acetic acid in absence and presence of inhibitors of 100-ppm concentration at 30 °C.

Inhibitor concentration (ppm)	$k10^{-3}$	$t_{1/2}$
20% formic acid	1.28±0.0608	538.46
AT	2.49±0.0029	278.87
AMT	1.95±0.0024	354.84
AET	1.59±0.0049	436.12
APT	1.75±0.0035	396.00
20% acetic acid	7.57±0.0089	91.49
AT	1.64±0.0019	421.79
AMT	1.34±0.0021	516.01
AET	1.17±0.0015	593.32
APT	0.71±0.0011	975.64

Application of the adsorption isotherm

The mechanism of corrosion inhibition may be explained on the basis of adsorption behaviour of the inhibitors [35]. The degrees of surface coverage (θ) for different inhibitor concentrations were evaluated from weight-loss data. Data were tested graphically by fitting to various isotherms. A plot of $\log \theta / (1 - \theta)$ vs. $\log C$ shows a straight line (Fig. 5a and 5b) indicating that adsorption follows the Langmuir isotherm

$$\theta / (1 - \theta) = k C \exp (- G_{\text{ads}}/RT) \quad (9)$$

where G_{ads} is the free energy of adsorption and C is the inhibitor concentration.

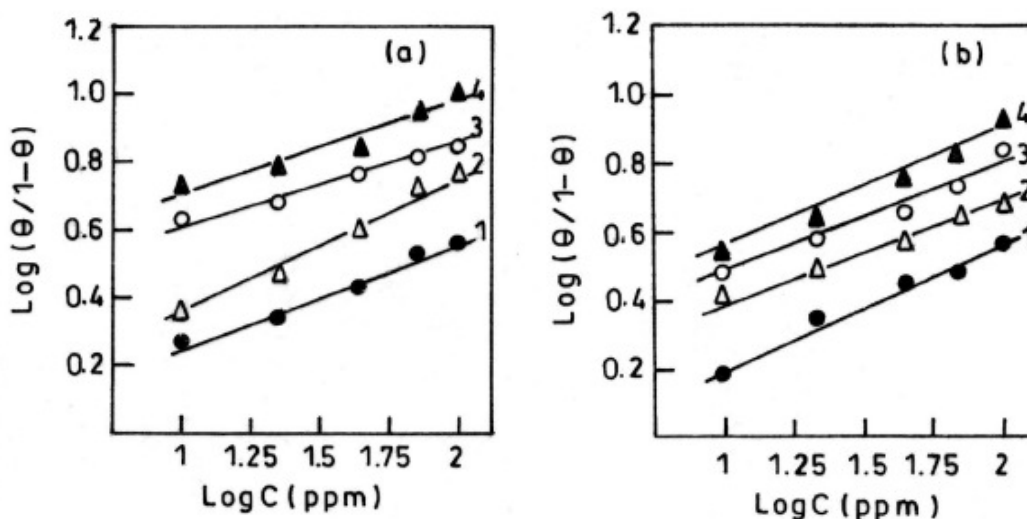


Figure 5. Langmuir's adsorption isotherm plots for the adsorption of various inhibitors on the surface of mild steel: a) 20% formic acid, b) 20% acetic acid (1: AT; 2: AMT; 3: AET; 4: APT).

Polarization measurements

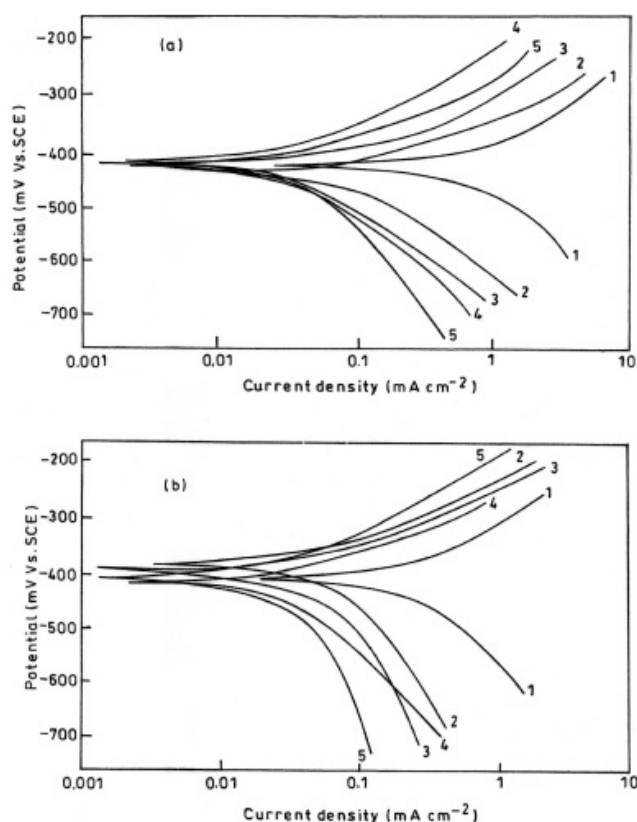
The cathodic and anodic polarization curves of mild steel in 20% formic and 20% acetic acid in the absence and presence of different inhibitors at 100-ppm concentration and at 28 ± 2 °C are shown in Fig. 6a and 6b. Electrochemical parameters such as corrosion current density (i_{corr}), corrosion potential (E_{corr}) and inhibition efficiency (IE) were calculated from Tafel plots and are given in Table 5. A maximum decrease in (i_{corr}) was observed for APT. It is also observed from Table 5, that (E_{corr}) values and Tafel slope constants b_a and b_c do not change significantly in inhibited solution as compared to uninhibited solution. It is seen from the results that thiadiazoles do not shift E_{corr} values significantly, thereby suggesting that they are mixed type inhibitors. This type of behaviour has been observed for mild steel in acid solution containing 2-hydrazino-6-methyl-benzothiazole [36].

Electrochemical impedance study

Impedance diagram obtained for mild steel in 20% formic acid is shown in Fig. 7 and the values of R_t , C_{dl} and % IE are given in Table 6. Values of R_t increase with increasing the inhibitor concentration and this in turn leads to an increase in the I.E [37]. There is lowering of C_{dl} values by the addition of 20% formic acid, suggesting that the inhibition can be attributed to the surface adsorption of the inhibitor on mild steel [38].

Table 5. Electrochemical polarization parameters for the corrosion of mild steel in 20% formic acid and 20% acetic acid containing 100 ppm inhibitors at 30 °C.

Inhibitor conc. (ppm)	E_{corr} (mV)	i_{corr} (mA cm^{-2})	IE (%)	b_a (mVdec^{-1})	b_c (mVdec^{-1})
20% formic acid	-416	0.350	—	68	104
AT	-420	0.068	80.57	62	120
AMT	-418	0.054	84.57	60	104
AET	-425	0.048	86.28	70	110
APT	-408	0.026	92.57	56	102
20% acetic acid	-404	0.240	—	60	100
AT	-385	0.052	78.33	52	92
AMT	-390	0.039	83.75	56	108
AET	-412	0.034	85.83	54	102
APT	-407	0.024	89.58	58	96

**Figure 6.** Potentiodynamic polarization curves for mild steel containing 100 ppm concentrations of various thiadiazoles in: a) 20% formic acid, b) 20% acetic acid (1: Blank; 2:AT; 3: AMT; 4: AET; 5: APT).

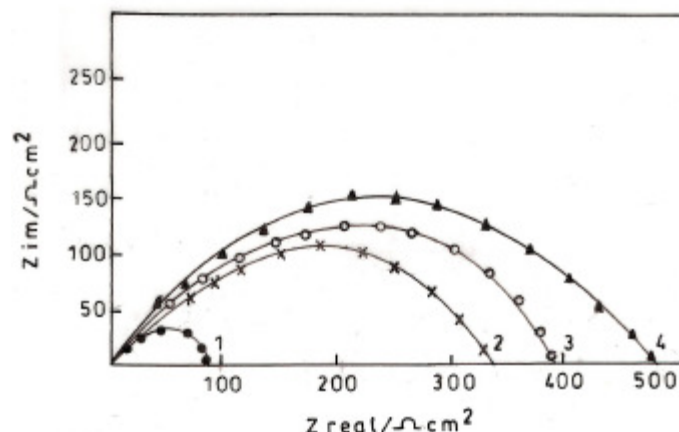


Figure 7. Electrochemical impedance diagram (Nyquist plot) for mild steel in the absence and presence of various concentrations of APT in 20% formic acid (1: Blank; 2: 10 ppm; 3: 50 ppm; 4: 100 ppm).

Table 6. Electrochemical impedance parameters for the corrosion of mild steel in 20% formic acid containing different concentrations of APT at 30 °C.

Concentration (ppm)	R_t (Ωcm^2)	C_{dl} ($\mu\text{F cm}^{-2}$)	IE (%)
20% formic acid			
Blank	75.00	1862.09	—
APT			
10	330.21	45.90	77.23
50	385.06	38.62	80.47
100	477.69	31.47	84.26

Scanning electron microscopy

SEM study (Fig. 8) shows that the inhibited metal surface is found to be smoother than uninhibited metal surface, because the inhibitor gets adsorbed by tightly binding on the metal surface, which shows less abrasion and corrosion on mild steel surface as compared to uninhibited metal surface.

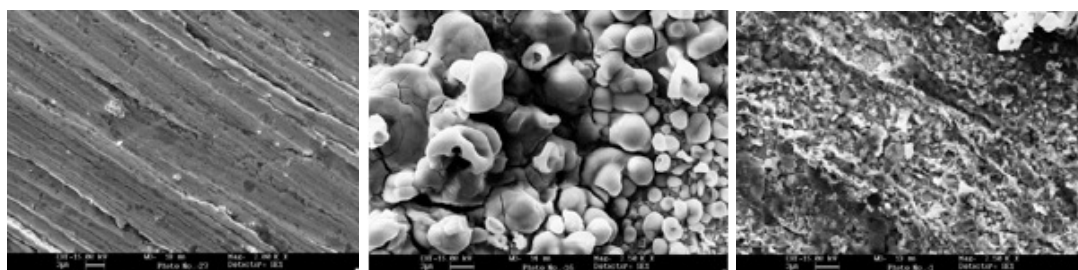
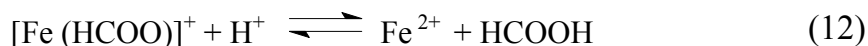


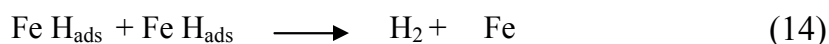
Figure 8. Scanning electron micrographs for: a) polished mild steel, b) mild steel in 20% formic acid, c) mild steel in 20% formic acid + 100 ppm APT.

Mechanism of corrosion inhibition

The corrosion of mild steel in non-aqueous and aqueous solution may occur in the following steps [39]:



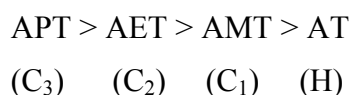
The evolution of hydrogen occurs due to the following cathodic reaction:



The adsorption of formate ions on the surface of iron is a prerequisite for the anodic dissolution to occur, thus the rate of corrosion should depend on the concentration of formate ion in the solution. The conductance of formic acid solution gradually increases in concentration range from 5% - 20%. As a result, the extent of adsorption of formate ion, as well as the rate of forward step (10), increases and consequently the rate of corrosion also increases.

The thiadiazoles inhibit the corrosion by controlling both the anodic and cathodic reactions. In acidic solutions these compounds exist as protonated species. These protonated species adsorb on the cathodic sites of the mild steel and decrease the evolution of hydrogen. The adsorption on anodic sites occurs through the π -electrons of aromatic rings and lone pair of electrons of nitrogen and sulphur atoms [35].

Among the compounds investigated, the order of IE is:



The presence of the propyl group in APT increases the density of electrons on the sulfur and nitrogen atoms caused by resonance effects, which facilitate stronger adsorption of APT on the mild steel surface. This leads to higher IE of APT than AET compared with AMT and AT. The IE decreases with decrease in the number of carbon atoms as a consequence of the decrease in the electron density on the nitrogen and sulfur atoms [40].

Conclusions

- (i) The thiadiazole derivatives showed good performance as corrosion inhibitors in formic acid and acetic acid media.
- (ii) Electrochemical study shows that the corrosion inhibition takes place by adsorption of the inhibitor on mild steel surface.

- (iii) All the compounds examined acted as mixed inhibitors in formic acid and acetic acid solutions.
- (iv) Scanning electron microscopy shows smoother surface of inhibited metal samples than inhibited samples due to the formation of a film on inhibited metal samples.
- (v) All of the four thiadiazoles inhibited corrosion by adsorption mechanism and the adsorption of these compounds from acid solution followed Langmuir's adsorption isotherm.

Acknowledgement

We acknowledge the Chairman, Department of Applied Chemistry, A.M.U, Aligarh, for providing the facilities needed in completing this work.

References

1. I.A. Sekine, A. Masuko and K. Senoo, *Corros. Sci.* 43 (1987) 553.
2. M.A. Quraishi and D. Jamal, *Corrosion* 56 (2000) 156.
3. V.B. Singh and R.N. Singh, *Corros. Sci.* 37 (1995) 1399.
4. I. Sekine, S. Hatakeyama and Y. Nakazawa, *Corros. Sci.* 27 (1987) 275.
5. E. Heitz, *Corrosion of Metals in Organic Solvents*, Plenum Press, New York, NY (1974) 226.
6. I. Sekine, H. Ohkawa and T. Hank, *Corros. Sci.* 22 (1982) 1113.
7. I. Sekine and A. Chinda, *Corrosion* 40 (1984) 95.
8. M.M. Singh and A. Gupta. *Mater. Chem. Phys.* 46 (1996) 15.
9. S. Muralidhara, M.A. Quraishi and S.V.K. Iyer, *Anti-Corros. Methods Mater.* 44 (1997) 100.
10. M.A. Quraishi, M.A.W. Khan and M. Ajmal, *Anti-Corros. Methods Mater.* 43 (1996) 5.
11. B. Hammouti, A. Aouniti, M. Taleb, M. Bright and S. Kertit, *Corrosion* 51 (1995) 411.
12. N. Al-Andis, E. Khamis, A. Al-Mayouf, and H. Aboul-Enein, *Corros. Prev. Cont.* 42 (1995) 13.
13. Abd-El-Nabey, E. Khammis, M.Sh. Ramadan and A.E. Gindy, *Corrosion* 52 (1996) 671.
14. E.M. Azhar, B. Mernari, M. Traisnel, F. Bentiss, M. Lagrenee, *Corros. Sci.* 43 (2001) 2229.
15. M. Bentiss, M. Traisnel and M. Lagrenee, *J. Appl. Electrochem.* 31 (2001) 41.
16. M. Lebrini, M. Lagrenee, H. Vezin, L. Gengembre and F. Bentiss, *Corros. Sci.* 47 (2005) 485.
17. F. Bentiss, M. Lebrini, H. Vezin, and Lagrenee, *Mater. Chem. Phys.* 87 (2004) 18.
18. F.A. Ansari and D. Jamal, *Mater. Chem. Phys.* 77 (2002) 687.
19. M. Kidwai, P. Misra, K.R. Bhushan and B. Dave, *Synth. Commun.* 30 (2000) 3031.

20. ASTM, Standard Practice for Laboratory Immersion Corrosion Testing of Metals, Annual Book of Standards, G 31-72, 3.02 (1990).
21. S.T. Hirozawa, Proc. 8th Eur. Symp. Corros. Inhi. Ann. Univ., Ferrara, Italy, 1 (1995) 25.
22. H. Ashassi-Sorkhabi, B. Shaabani, D. Seifzadeh, *Electrochim. Acta* 50 (2005) 3446.
23. K. Juttner, *Electrochim. Acta* 35 (1990) 1501.
24. L.J. Jha, Faculty of Science, Delhi University, Delhi, Ph.D. Thesis (Studies of the adsorption of amide derivative during acid corrosion of pure iron and its characterization) (1990) 111.
25. C.B. Breslin and W.M. Carrol, *Corros. Sci.* 34 (1993) 327.
26. M.G.A. Khedr and M.S. Lashien, *Corros. Sci.* 33 (1992) 137.
27. S.S.A. Rehim, H.H. Hassan, M.A. Amin, *Mater. Chem. Phys.* 70 (2001) 64.
28. I.N. Putilova, S.A. Balezin and Baranik, *Metallic Corrosion Inhibitors* (Pergamon Press, New York), (1960) 31.
29. M.K. Gomma and M.H. Wahdan, *Mater. Chem. Phys.* 39 (1995) 209.
30. M. Schorr and J. Yahalom, *Corros. Sci.* 12 (1972) 867.
31. B.G. Ateya, B.E. Andouli and F.M. Nizami, *Corros. Sci.* 24 (1984) 509.
32. G.K. Gomma and M.H. Wahdan, *Indian J. Chem. Technol.* 2 (1995) 107.
33. K. Orubite-Okorosaye and N.C. Oforka, *J. Appl. Sci. Environ.* 8 (2004) 57.
34. P.W. Atkins, *Chemisorbed and physisorbed species, a textbook of physical chemistry* (University press, Oxford), (1980) 936.
35. M.A. Quraishi, A.S. Mideen, M.A.W. Khan and M. Ajmal, *Indian J. Chem. Technol.* 1 (1994) 329.
36. M. Ajmal, A.S. Mideen and M.A. Quraishi, *Corros. Sci.* 36 (1994) 79.
37. M. Houyi, S. Chen, B. Yin, S. Zhao, X. Liu, *Corros. Sci.* 45 (2003) 867.
38. N.C. Subramaniyam, S. Mayanna, *Corros. Sci.* 25 (1985) 163.
39. M.M. Singh and A. Gupta, *Mater. Chem. Phys.* 46 (1996) 15.
40. M.A. Quraishi and S. Khan, *J. Appl. Electrochem.* 36 (2006) 539.